Scaling Relationships of Dissipation-Induced Pavement–Vehicle Interactions

SCALING RELATIONS OF DISSIPATION-INDUCED PAVEMENT-VEHICLE INTERACTIONS

By: A. Louhghalam[1], M. Akbarian[2], F.-J. Ulm[3]

Submission Date: July 2, 2013

Revised Paper Submission Date: Nov 12, 2013

Final Submission Date: Feb 8, 2014

Word Count: 4687 + 7 Figures + 3 Tables = 7187

Affiliation/Address:

[1]Arghavan Louhghalam,
Department of Civil & Environmental Engineering
Massachusetts Institute of Technology
Cambridge MA 02139
Email: arghavan@MIT.EDU

[2]Mehdi Akbarian
Department of Civil & Environmental Engineering
Massachusetts Institute of Technology
Cambridge MA 02139
Email: akbarian@mit.edu

[3]Franz-Josef Ulm (Corresponding Author)
Department of Civil & Environmental Engineering
Massachusetts Institute of Technology
Bldg. 1-263
77 Massachusetts Avenue
Cambridge MA 02139
Tel: 617-253.3544
Emails: ulm@mit.edu

Abstract: Rolling resistance is one of the key factors that affect the fuel efficiency of the national pavement system. Beside pavement texture and pavement roughness, the dissipation of mechanical work provided by the vehicle due to viscous deformation within the pavement structure has been recognized as a relevant factor contributing to the environmental footprint of pavement systems. This dissipation depends on material and structural parameters that can be optimized in order to increase the fuel efficiency of pavements. Identifying the key material and structural parameters that drive this dissipation, is in short the focus of this paper. This is achieved by a combination of dimensional analysis and model-based simulations of the dissipation of a viscoelastic beam on elastic foundation. It is found that for linear viscoelastic systems, the dissipation scales with square of the vehicle weight, with the inverse of the viscous relaxation time; in addition to distinct power relations of top layer stiffness, thickness and subgrade modulus. These scaling relations can be used by pavement engineers to reduce such pavement-inherent dissipation mechanisms, and thus increase the fuel efficiency of a pavement design. By way of example, we show the application of these scaling relations with data extracted from FHWA's Long Term Pavement Performance (LTPP) database for seven road classes. We show that the scaling relations provide a means to evaluate the performance of the different road classes in terms of their fuel efficiency related to dissipation.

INTRODUCTION

The overall need to enhance the sustainability of our pavement system requires quantitative engineering models that relate pavement structure, pavement condition and materials to rolling resistance, fuel consumption and related greenhouse gas emissions. Beside pavement texture and pavement roughness, the dissipation of mechanical work provided by the vehicle due to viscous deformation within the pavement structure has been recognized as a relevant factor contributing to the rolling resistance some 40 years ago. In fact, in his famous book "Viscoelasticity" (*1*), in conclusion of his analysis of the viscoelastic response of a Kelvin beam on elastic foundation to a moving load, showing that the vehicle load is on an upward slope, Wilhelm Flügge notes that "the load moving with the velocity c has to do work", and that the associated horizontal force "supplies the energy needed for the viscoelastic deformation". He continues that "this phenomenon, well known and occurring in various situations, does not stand in common text books". - The phenomenon has indeed been observed both experimentally and theoretically in many pavement and railroad mechanics studies (*2-4*); but gained some new attention more recently in the context of the development of engineering methods for the sustainable design of pavements, accounting and eventually reducing the generation of greenhouse gas (GHG) emissions during the use phase of pavements (*5-7*), especially for roads with high traffic volume. In contrast to the impact of roughness-induced Pavement-Vehicle Interactions (PVI) that depend primarily on vehicle characteristics (*8*), the fuel-consumption excess due to viscous energy dissipation depends on material and structural parameters that can be influenced by the pavement engineer. With this focus in mind, this contribution aims at deriving scaling relations from a combination of dimensional analysis and model-based simulations of a simple viscoelastic beam model.

THEORETICAL BACKGROUND

To motivate the forthcoming development, consider a pavement structure subjected to a load P moving at a constant speed c in the x-direction (Fig. 1). For any irreversible deformation that takes place in the pavement structure, energy is dissipated, which needs to be compensated by additional vehicle power; and thus fuel consumption. There are a priori two ways of evaluating the dissipation rate $\mathcal{D}$; that is the amount of work rate δW which is not stored into recoverable (elastic) energy, but dissipated into heat form. One approach is based on using a fixed reference frame. This approach employed e.g. by Pouget et al. (*5*), typically employs finite elements for estimating the time-history of the displacement field in a sufficiently large block of pavement (to minimize the effects of boundary conditions). Using classical finite element procedure, stresses and viscoelastic strains are determined; and the dissipated energy is obtained by integrating over the entire pavement system. The second approach considers a moving coordinate frame that moves at the speed of the vehicle. In the vein of Flügge's conjecture, it is realized that due to the presence of a dissipative mechanism in the system, the vehicle is always on an uphill slope, leading to an additional horizontal force supplied by the vehicle, that is added to the rolling resistance, and thus to fuel consumption. The dissipation rate $\mathcal{D}$ in this approach is obtained from writing the external work rate of the force in the moving coordinate system, $X = x - ct$, where x and t

are space and time variables in the fixed coordinate system and by assuming steady state conditions under constant speed c (i.e., Lagrangian derivative, $\partial(.)/\partial t = -c\,\partial(.)/\partial X$); so that (see, e.g. (*6,9*)):

$$\mathcal{D} = \delta W = P\frac{dw}{dt} = -cP\frac{dw}{dX} \geq 0 \quad (1)$$

where δW is the external work rate, and P is the axel load, w is the deflection at the point of load application, and dw/dX the slope. Hence, for the case of an elastic material with no dissipation, the slope is $dw/dX = 0$, which means that the tire is at the bottom of the deflection basin. However, if dissipation occurs in the pavement structure (for instance, due to viscous deformation mechanisms), the non-negativity of the dissipation, Eq. (1), requires that $dw/dX < 0$. This is precisely Flügge's conjecture which he based on solving the viscoelastic beam problem (*1*), but which is in fact a thermodynamic requirement: "Where the load is applied, the beam has an upward slope" (Fig. 1). For practical purposes, it is often more useful to translate the dissipation rate $\mathcal{D}$ (of dimension Energy/Time) into the amount of excess energy per pavement length the vehicle needs to spend to maintain constant velocity. This is achieved by dividing $\mathcal{D}$ by c; that is:

$$\delta E = \mathcal{D}/c = -P\frac{dw}{dX} \quad (2)$$

This approach, which considers the slope as added grade, has been used in (*7*), and is often referred to as “deflection-induced” PVI-approach. It is, however, strictly equivalent to the so-called dissipation-induced PVI approach. In a previous work (*7*) devoted to a first-order estimate of the dissipation, we estimated the slope dw/dX from the maximum deflection of a beam on a viscoelastic foundation, using $dw/dX \approx w_{max}/(\pi\ell_s)$, where $\ell_s = (\frac{Eh^3}{12}/k)^{1/4}$ is the Winkler length (with E the Young's modulus, h the top layer thickness, k the subgrade modulus). This approach, though simple, failed to capture both the velocity and temperature dependence of the rolling resistance as shown in some studies. In this contribution, we explicitly address this issue, by considering the viscoelastic response of the top layer. By doing so, we will address the question, how the dissipation rate, as expressed by Eq. (1), scales with material and structural properties of the pavement.

DIMENSIONAL ANALYSIS

A convenient way to screen possible invariants of material and structural parameters is to perform a dimensional analysis. To reduce the complexity of the pavement system, we consider the dissipation rate of a viscoelastic beam of width b on an elastic foundation (subgrade modulus k) subjected to a moving load P. The beam's elastic response is described by the Winkler length, $\ell_s = (\frac{Eh^3}{12}/k)^{1/4}$, while the viscoelastic response is captured by a relaxation time $\tau = \eta/E$. The constant speed c at which the load moves is smaller than the critical velocity $c_{cr} = \ell_s(k/m)^{1/2}$ (with $m = \rho h$ the surface mass density, $\rho =$ volume mass density), which is close to a multiplying factor the critical resonant frequency. For the dimensional analysis, we are thus interested in a relation between dissipation rate, $\mathcal{D}$, two load parameters (P, c), and five material-structural parameters:

$$\mathcal{D} = f(P, c, b, \ell_s, k, c_{cr}, \tau) \tag{3}$$

where b and τ are beam width and relaxation time of the viscoelastic top layer respectively. For the dimensional analysis, we adopt an extended base dimension system that renders an account of the difference of dimensions in different direction (*9*). In this system, we express all quantities involved in Eq. (2) in an $L_xL_yL_zMT$- base dimension system, where L_i stands for the length dimension L in the $(i = x, y, z$ – directions. For instance, the load P is applied in the z-direction, and has thus as dimension function, $[P] = L_zMT^{-2}$. Similarly, in this base dimension system, $[c] = [c_{cr}] = L_xT^{-1}$; $[b] = L_y$; $[\ell_s] = L_x$; $[k] = (L_xL_y)^{-1}MT^{-2}$ and $[\tau] = T$. In its turn, for the determination of the dimension function of dissipation $\mathcal{D}$ we use expression (1), that is $[\mathcal{D}] = [c][P][w]/[X] = L_z^2MT^{-3}$. We summarize the dimension functions in form of the exponent matrix of dimension:

$$\begin{vmatrix} L_x \\ L_y \\ L_z \\ M \\ T \end{vmatrix} \begin{vmatrix} [\mathcal{D}] & [P] & [c] & [b] & [\ell_s] & [k] & [c_{cr}] & [\tau] \\ 0 & 0 & 1 & 0 & 1 & -1 & 1 & 0 \\ 0 & 0 & 0 & 1 & 0 & -1 & 0 & 0 \\ 2 & 1 & 0 & 0 & 0 & 0 & 0 & 0 \\ 1 & 1 & 0 & 0 & 0 & 1 & 0 & 0 \\ -3 & -2 & -1 & 0 & 0 & -2 & -1 & 1 \end{vmatrix} \tag{4}$$

The rank of the matrix is $k = 5$, which allows us, according to the Pi-Theorem (*10*), to reduce the dimensional relation (3) of $N + 1 = 8$ parameters to $N + 1 - k = 2 + 1$ dimensional relation. That is, if we choose $(P, b, \ell_s, k, c_{cr})$ as dimensionally independent parameters, we can express the remaining ones as power functions of the former in a dimensionless form as follows:

$$\Pi = \frac{\mathcal{D}\ell_s^2 bk}{P^2 c_{cr}} = F\left(\Pi_1 = \frac{c}{c_{cr}}; \Pi_2 = \frac{\tau c_{cr}}{\ell_s} = \zeta\right) \tag{5}$$

or in terms of the excess energy consumption $\delta E = \mathcal{D}/c$:

$$\Pi = \frac{\delta E\, \ell_s^2 bk}{P^2}\frac{c}{c_{cr}} = F\left(\Pi_1 = \frac{c}{c_{cr}}; \Pi_2 = \frac{\tau c_{cr}}{\ell_s} = \zeta\right) \tag{6}$$

where $\zeta = \tau(k/m)^{1/2}$ is the damping ratio. A first observation from Eqs. (5) and (6) is that the excess energy scales as $\mathcal{D} \propto P^2$. That is, if a force, P_0 (i.e. axle load or vehicle mass), is increased by a factor λ such that $P = \lambda P_0$, the dissipation rate, respectively the excess energy, is increased by $\mathcal{D} = \lambda^2\mathcal{D}_0$. Other scaling relations though require a solution of the dimensionless function F; as shown here below.

Finally, it is worth mentioning that from a dimensional analysis point of view, the dimensionless scaling relations (5) and (6) still hold for an elastic beam on a viscoelastic foundation, which we considered in an earlier contribution (*7*). On the other hand, by considering the distinct viscoelastic behavior of the top layer, it is possible to factor into the scaling of dissipation related fuel consumption environmental effects, such as the dependence of the materials' relaxation time on temperature (*5-6*). This is shown later on.

MODEL-BASED SIMULATIONS OF DISSIPATION DUE TO PVI

Herein, we use model-based simulations of a viscoelastic beam on elastic foundation (Fig. 2a). Since our focus is on first-order scaling relations of the dissipation in terms of the dimensionless expression (5), we employ the most simple viscoelastic model, namely a linear viscoelastic Maxwell model of an elastic spring (stiffness E), in series with a dashpot (viscosity η), that define the relaxation time $\tau = \eta/E$ (Fig. 2b) For the beam problem, we recall the equation of motion for an infinite elastic beam on an elastic foundation in a moving coordinate system (see e.g. (*11-12*) among many other references):

$$EI\left(\frac{\partial^4 w}{\partial X^4}\right) + mc^2\left(\frac{\partial^2 w}{\partial \bar{X}^2}\right) + kw = \frac{P}{S_c} \tag{7}$$

where $I = h^3/12$ and S_c is the tire-pavement contact area ($p = P/S_c$ is the contact pressure which in the moving coordinate system is a constant). Taking the Fourier transform of this differential equation yields:

$$\widehat{w} = \hat{p}(EI\lambda^4 - mc^2\lambda^2 + k)^{-1} \tag{8}$$

where λ is the transformed field of X. To evaluate the deflection of a viscoelastic beam, we employ the elastic-viscoelastic correspondence principle (*13-14*), and substitute the complex modulus for its elastic counterpart in Eq. (7). For a Maxwell material with the constitutive equation relating the components of stress σ and strain ε, $(\sigma + \tau\dot{\sigma})/E = \tau\dot{\varepsilon}$, we have in the moving reference frame, $(\sigma - c\tau\, d\sigma/dX)/E = -c\tau d\varepsilon/dX$. Then, taking the Fourier transformation, i.e. $\hat{\sigma}(1 - c\tau\, i\lambda)/E = -c\tau i\lambda\hat{\varepsilon}$ (with i the imaginary unit), the complex modulus is obtained $\widehat{E}\,/E = -i\lambda c\tau/(1 - ic\tau\lambda)$; whence, instead of the viscoelastic solution in Fourier domain:

$$\widehat{w} = \frac{\hat{p}}{k}\left(\frac{-i\bar{c}\,\zeta\,\bar{\lambda}}{(1-i\bar{c}\,\zeta\,\bar{\lambda})}\bar{\lambda}^4 - \bar{c}^2\bar{\lambda}^2 + 1\right)^{-1} \tag{9}$$

where $\bar{\lambda} = \ell_s\lambda$, while $\bar{c} = c/c_{cr}$ and $\zeta = \tau(k/m)^{1/2}$ are the invariants identified from dimensional analysis in Eq. (5). The dissipation rate is then directly obtained from Eq. (1) by inverse Fourier transformation ($\mathcal{F}^{-1}$):

$$\mathcal{D} = -cP\frac{dw}{dX} = -cP\mathcal{F}^{-1}(i\lambda\widehat{w})|_{X=0} \geq 0 \tag{10}$$

or, in terms of excess energy consumption, Eq. (2):

$$\delta E = \mathcal{D}/c = -P\mathcal{F}^{-1}(i\lambda\widehat{w})|_{X=0} \geq 0 \tag{11}$$

By way of application, Fig. 2c displays the deflection field for a viscoelastic beam obtained from the inverse Fourier transform of Eq. (9).

SCALING OF DISSIPATION-INDUCED FUEL CONSUMPTION

Figure 3a displays, in the dimensionless form (5), the dissipation in function of the normalized velocity, $\Pi_1 = c/c_{cr}$, for three fixed damping ratios, $\Pi_2 = \zeta = \tau(k/m)^{1/2} = 1$, 5, 10. Remarkably, for a given

value of ζ (and thus relaxation time, after a first sharp increase at low velocity values, the dimensionless dissipation is almost constant over a wide range of velocities, $\Pi_1 = c/c_{cr}$, before increasing to a vertical asymptote at the critical velocity. In return, as shown in Figure 3b, for a given normalized velocity c/c_{cr}, the dissipation rate decreases as the damping ratio, and hence the viscous relaxation time τ, increases. This means, as expected, that the faster the rate of viscous deformation (and thus the smaller τ), the greater is the dissipation rate.

Given these results, for a first-order back-of-the-envelope engineering estimate, the dissipation rate (respectively the excess energy consumption) scales, for a wide range of relevant velocities, $0.2 < \frac{c}{c_{cr}} < 0.8$, with the viscous relaxation time τ, vehicle load P, top layer stiffness E, top layer thickness h, and subgrade modulus k as:

$$\mathcal{D} \propto \tau^{-1} \times P^2 \times E^{-1/4} \times h^{-3/4} \times k^{-1/4} \tag{12}$$

or in terms of the excess energy consumption:

$$\delta E = \mathcal{D}/c \propto (c\tau)^{-1} \times P^2 \times E^{-1/4} \times h^{-3/4} \times k^{-1/4} \tag{13}$$

It is interesting to note that the scaling relations of dissipation rate and excess energy consumption are consistent with a recent North American calibration of the World Bank's HDM-4 model for vehicle operating costs (*15*), that reported statistically significant effects of surface texture for heavier trucks (i.e. $\delta E \propto P^2$) and at low speed (i.e. $\delta E \propto c^{-1}$).

Evaluating the dissipated energy using (11) is complex and therefore not appropriate for engineering purposes (see (*9*) for the detailed method and calculations). For practical use, we fitted the log of dimensionless expression (5) (Fig. 3c) to a two-dimensional surface that fits very well the discrete data (Fig. 3d) for $0.03 < c/c_{cr} < 0.5$ and $0.0001 \leq \zeta \leq 12{,}000$.

$$\log_{10}(\Pi) = \log_{10} \frac{\mathcal{D}\ell_s^2 bk}{P^2 c_{cr}} = \log_{10} F\left(\Pi_1 = \frac{c}{c_{cr}}; \Pi_2 = \zeta\right) = \sum_{i=0}^{i=5} \sum_{j=0}^{j=3} p_{ij} {\Pi_1}^i \times \log_{10}(\Pi_2)^j \tag{14}$$

Coefficients p_{ij} (coefficient of determination of $R^2 = 0.972$) are tabulated in Table 1. Having the material and structural properties of a pavement in hand, one can use (14) to readily evaluate the dissipated energy and fuel consumption. This approach is used herein to evaluate the fuel consumption in the United States roadway network.

EFFECT OF TEMPERATURE ON DISSIPATION

A simple means of accounting for the temperature dependence of the viscoelastic response is by employing –analogous to the Arrhenius concept– the activation energy concept for the relaxation time:

$$\tau(T) = \tau\left(T_{ref}\right) \times a_T(T) \tag{15}$$

where $a_T(T)$ is the shift factor accounting for the acceleration or deceleration of the relaxation time when the temperature T is different from a reference temperature T_{ref}. For concrete, the classical activation energy concept has been shown to hold (*16*):

$$\log a_T(T) = U_c \left[\frac{1}{T} - \frac{1}{T_{ref}}\right] \quad (16)$$

with $U_c = 2{,}700$ K. [Temperatures reported in Kelvin.] In return, for asphalt mixes, following the suggestion in (*5*), the William, Landel, and Ferry law (*17*) has shown to capture well the time shift:

$$\log a_T(T) = \frac{-C_1(T-T_{ref})}{C_2+(T-T_{ref})} \quad (17)$$

where C_1, C_2 are empirical constants. Typical values for bituminous asphalt mixes reported in (*5*) are $C_1 = 34$ and $C_2 = 203$ K for a reference temperature of $T_{ref} = 283$ K (10°C).

MODEL CALIBRATION-VALIDATION

In contrast to previous approaches, the model here presented requires as input the characteristic relaxation time, $\tau(T_{ref})$, representative of the viscoelastic response of the constituent material. To calibrate the model, we consider results reported in (*5*), in which the dissipated energy in an asphalt concrete layer subjected to a moving truck of 40 tons on three axles as illustrated in Figure 4a was calculated, by means of finite elements, considering a generalized Kelvin chain to represent asphalt's viscoelastic response, at different temperatures and two speeds, $c = 100$ km/h and $c = 50$ km/h. We model the same pavement structure and material properties by means of a viscoelastic beam-model representation: $E = 40{,}114$ MPa, $h = 0.22$ m, and $k = 35$ MPa/m. In determining the subgrade modulus, we use an empirical relation developed in (*18*), that links the subgrade elastic modulus E_s to the subgrade stiffness $k = \alpha E_s$, where $\alpha = 0.29/\mathrm{m}$. The model calibration-validation is done in two steps:

- Calibration: For the calibration, we consider the reported dissipated energy values for $c = 100$ km/h at different temperatures (10,30,40,50,55,60°C). By minimizing the quadratic error between our model predictions and the model predictions reported in (*5*), we calibrate the relaxation time, $\tau(T_{ref} = 10°\mathrm{C}) = 0.0083$ s. The fit is shown in Figure 4b.
- Validation: For the validation, we compare our model predictions with the reported dissipated energy values for $c = 50$ km/h at different temperatures (40,60°C). This comparison is shown in Figure 4c.

The successful validation-calibration shows that the model herein presented is able to capture the sensitivity of the pavement's material-structural response to both temperature and speed. Given the simplicity of the model (a Maxwell model), this may be on first sight surprising. On the other hand, at typical vehicle speeds the characteristic time of loading of the material is relatively short; so that one viscous relaxation time may well be sufficient to capture the viscous response for the estimation of the

dissipated energy in a moving coordinate frame. Further validation based on measuring the energy dissipation due to moving load at different temperature and speed is still required to confirm this conjecture, and will be reported in the future.

APPLICATION OF SCALING WITH LTPP DATA BASE

By way of application, we apply the model with data extracted from FHWA's Long-Term Pavement Performance (LTPP) program (*19*). Specifically, we consider here the data available through the General Pavement Studies (GPS) program, recorded from in-service pavement test sections in either their original design phase or in their first overlay phase (*19*). Under the GPS program, more than 800 test sections were established on in-service pavements in all 50 States and in Canada. The GPS sections generally represent pavements that incorporate materials and structural designs used in standard engineering practices in the United States and in Canada. Each GPS section is 152 m (500 ft) in length and is located in the outside traffic lane. The data collected at the GPS sections include: climatic, material properties, traffic frequency, deflection profile, distress, and friction data. The GPS section categories considered in our investigation are listed in Table 2.

Input Data

For each GPS section class, we determine distribution of top layer thickness h, top layer stiffness E, and subgrade modulus k, using a consistent calibration–validation method described in details in (*7*) which involves for each section:

- Calibration of (E, k) using wave propagation characteristics of Falling Weight Deflectometer time history data recorded by FHWA's LTPP program.
- Validation of calibrated (E, k) data against deflection values from the FWD tests at various distances from the loading point.
- Comparison of our values with top layer and subgrade modulus values reported in the LTPP database.

The distribution of top layer modulus E, subgrade stiffness and top layer thickness are displayed in Figure 5 for the two AC pavement systems (GPS-1, GPS-2), PCC systems (GPS-3, GPS-4, GPS-5), and composite systems (GPS-6, GPS-7). The general trend is that the distributions are log-normal. The ln-Mean and standard deviations are provided in Table 3. As detailed below, these distributions are the input for Monte-Carlo simulations of dissipation-induced PVI. In return, for purpose of comparison, we assume for all GPS-systems, the same relaxation time, $\tau\left(T_{ref} = 10°\mathrm{C}\right) = 0.0083$ s.

Monte-Carlo Approach

A Monte-Carlo approach is implemented to evaluate, for each GPS section category in the LTPP data set and a given vehicle class (i.e. axle load P), the excess energy consumption from Eq. (6); that is:

$$\delta E = \mathcal{D}/c = \frac{P^2}{\ell_s^2 b} \times \frac{c_{cr}}{c} \times F\left(\Pi_1 = \frac{c}{c_{cr}}; \Pi_2 = \zeta = \tau(k/m)^{1/2}\right) \quad (15)$$

where the value of the dimensionless dissipation rate, $\Pi = F(\Pi_1, \Pi_2)$, is estimated from Eq. (14).

In the Monte-Carlo Simulations, for each GPS section type, the distributions of top layer stiffness, top layer thickness and subgrade modulus are considered, to estimate the distribution of the excess energy consumption. In addition, in the Monte-Carlo simulations, we can as well consider seasonal temperature variations, by considering the annual mean temperature and the standard variation.

The Monte-Carlo approach is based on the ergodicity principle: the average values over time of physical quantities (here dissipated energy) that characterizes a system (here pavement) are equal to the statistical average values of the same quantities realized by a large amount of possible configurations (*20*). In this sense, the Monte-Carlo approach is well suited to capture the excess-energy consumption of the network represented by the LTPP database.

Results

Figures 6a-c display the dissipated energy of an HS20-44 truck shown in Figure 4a with axle loads $P_1 = 36.29$ kN (8,000 lbs), $P_2 = P_3 = 145.15$ kN (32,000 lbs) at a constant speed $c = 100$ km/h and a temperature $10℃ \pm 10℃$, for the seven GPS section types, regrouped for purpose of comparison in three categories: Asphalt Concrete Pavements (GPS-1, GPS-2, Fig. 6a), Concrete Pavement (GPS-3, GPS-4, GPS-5, Fig. 6b), and Composite Pavement structures (GPS-6, GPS-7, Fig. 6c). Not surprisingly, given the log-normal distribution of the input parameters, the excess energy due to dissipation follows as well a log-normal distribution. The following observations deserve attention:

- For asphalt concrete pavements (Fig. 6a), we recognize a statistically significant effect of the subgrade on the dissipated energy: a stabilized base can reduce the dissipated energy on-average by 25% compared to a granular base. In return, the distribution of the dissipated energy is wide for both GPS-1 and GPS-2, spanning more than three orders of magnitude.
- The dissipated energy of concrete pavement structures (Fig. 6b) exhibits a very narrow distribution, and is almost insensitive to the presence of joints and reinforcement (GPS-3, GPS-4, GPS-5).
- Composite sections (Fig. 6c) achieve a peak distribution similar to concrete pavements; albeit with a wider distribution, reminiscent of the one of asphalt pavements. There is a statistically significant difference between GPS-6 and GPS-7, that relates to the stiffness of the pavement on which the asphalt overlay is built (asphalt concrete for GPS-6, PCC for GPS-7).

The results so far presented considered a constant speed of $c = 100$ km/h and a moderate temperature, $10℃ \pm 10℃$ (mean $\pm$ standard deviation). To show the impact of both a varying speed and temperature, Figure 7 displays the dissipated energy in function of temperature and speed, for three of the seven GPS-systems. To account for the difference in distributions, the dissipated energy is evaluated at the 95% confidence level. As expected, the specific temperature and rate sensitivity of the top-layer material translates into a sensitivity of the dissipated energy.

CONCLUSIONS

The need to enhance the sustainability of our pavement system requires quantitative engineering models capable to capture – at least in first order – the impact of pavement structure and constitutive materials on fuel consumption and related greenhouse gas emissions. The model presented herein, which refines our previous work (*7*), aims at just this. The following points deserve attention:

1. In order to maintain a constant speed, the vehicle's engine needs to supply additional energy to compensate for the energy that is dissipated in the pavement structure. This excess energy depends on structural and material properties of the pavement, temperature and vehicle speed.

2. The complexity of the viscoelastic phenomena involved can be reduced to a few dimensionless quantities that combine materials and structural parameters. In this dimensionless space, the excess energy demand can be evaluated by means of mechanistic models. Herein, we have chosen the simplest model, a viscoelastic beam on an elastic foundation, to capture the dissipative response of the system in a dimensionless form that can be easily used for first-order evaluations of the dissipated energy. The dimensionless form, however, can also be used together with other more comprehensive models based on plate theory or continuum theory that are currently in development. Note that in the model developed herein it is assumed that the pavement material is viscoelastic. That is, while the energy dissipation is temperature dependent due to the viscous component of the pavement model, no irreversible deflection is considered. Otherwise said, the dissipation of energy due to the plasticity of the pavement arising in extreme temperature and stress levels is not taken into account.

3. Beside elastic and structural data that are (mostly) readily available, the model requires calibration of a viscous relaxation time. Herein, we calibrated this relaxation time for asphalt against literature data. Further research is needed here to link this relaxation time to classical material test results. Fortunately, given the relatively short residence time of a moving vehicle on a specific place, it appears to us that not the entire frequency domain is required to capture the time-dependent response of the constituent materials.

4. The application of the model with data from the LTPP data base shows that the dissipation and its distribution are temperature, speed and material dependent. Thus, for a chosen or given pavement structure, it becomes possible to evaluate the excess fuel consumption with a

minimum of material and structural parameters, and use the dissipated energy as a design criterion for minimizing the carbon footprint of our pavement system.

In summary, while certainly small for a single vehicle, the increasing average annual daily truck traffic (AADTT) adds up to a significant amount of excess fuel consumption. For instance, considering AADTT=10,000 (an average value representative of the traffic volume of the GPS pavement systems), together with EPA's MPGe rating (according to which 1ltr of fuel equates to 32.05 MJ), the total energy dissipated per day at the 95% confidence level amounts to 178-468 ltr/km of excess fuel consumption per day for GPS-1, 11-38 ltr/km for GPS-3 and 44-139 ltr/km for GPS-7, with the lower value corresponding to $c = 100$ km/h and $10℃$, and the upper value to either lower speeds ($c = 20$ km/h and $10℃$), or higher temperature ($c = 100$ km/h and $20℃$). That is, there are significant opportunities for reducing the environmental impact of our pavement system.

ACKNOWLEDGMENT: This research was carried out by the CSHub@MIT with sponsorship provided by the Portland Cement Association (PCA) and the Ready Mixed Concrete (RMC) Research & Education Foundation. The CSHub@MIT is solely responsible for content.

REFERENCES

1. Flügge, W. *Viscoelasticity*. Springer Verlag, New York, Heidelberg, Berlin, 2nd Revised Edition, 1975, pp. 92-93.
2. Greenwood Engineering traffic speed deflectometer *www.greenwood.dk/TSD/default.asp, 2008*
3. Kim, S. M., Roesset , J. M. Moving loads on a plate on elastic foundation. *Journal of Engineering Mechanics*, Vol. 124, 1998, pp 1010-1017
4. Kim, S. M., Roesset , J. M. Dynamic response of a beam in a frequency-independent damped elastic foundation to moving load. *Canadian Journal of Civil Engineering*, Vol. 30, No. 2, 2003, pp 460-467
5. Pouget, S., Sauzéat, C., Di Benedetto, H., and Olard, F. Viscous Energy Dissipation in Asphalt Pavement Structures and Implication for Vehicle Fuel Consumption. *Journal of Materials in Civil Engineering*, Vol. 24, No. 5, 2012, pp. 568-576.
6. Chupin, O., Piau, J.-M., and Chabot, A. Evaluation of the structure-induced rolling resistance (SRR) for pavements including viscoelastic material layers. *Materials and Structures*, Vol. 46, 2013,pp. 683–696.
7. Akbarian, M., Moeini-Ardakani, S.S., Ulm, F.-J, and Nazzal, M. Mechanistic Approach to Pavement–Vehicle Interaction and Its Impact on Life-Cycle Assessment. *In Transportation Research Record: Journal of the Transportation Research Board, No. 2306*, Transportation Research Board of the National Academies, Washington, D.C., 2013, pp. 171–179.
8. Zaabar, I., and K. Chatti. Calibration of HDM-4 Models for Estimating the Effect of Pavement Roughness on Fuel Consumption for U.S. Conditions. In *Transportation Research Record: Journal of the Transportation Research Board, No. 2155*, Transportation Research Board of the National Academies, Washington, D.C., 2010, pp. 105–116.

9. Louhghalam, A., Akbarian, M., and Ulm, F.-J. Fluegge's Conjecture: Dissipation vs. Deflection-induced Pavement Vehicle Interactions. *Journal of Engineering Mechanics*, *under review,* 2013.
10. Buckingham, E. On physically similar systems; illustrations of the use of dimensional equations. *Physical Review,* Vol 4, 1914, pp. 345–376
11. Kelly, J. M. Moving load problems in the theory of viscoelasticity. PhD thesis Dept. of Civil Engineering, 1962.
12. Fryba, L. *Vibration of solids and structures under moving loads.* Thomas Telford, 1999.
13. Christensen, R. *Theory of viscoelasticity: an introduction.* Academic press, 1982.
14. Read, W. T. Stress analysis for compressible viscoelastic materials. *Journal of Applied Physics,* Vol. 21, No. 7, 1950, pp. 671-674.
15. Chatti, K., Zaaber, I. *Estimating the effects of pavement condition on vehicle operating costs.* NCHRP Report 720. Transportation Research Board of the National Academies, Washington, D.C., 2012.
16. Bazant, Z.P. Creep and damage in concrete. Materials science of concrete, J. Skalnet and S. Mindess, eds. *American Ceramic Society*, Westerville, Ohio, 1980, 335–389.
17. Ferry, J. D. *Viscoelastic properties of polymers*, John Wiley & Sons, Chichester, 1980.
18. Khazanovich, L., Tayabji, S. D., and Darter, M. I. *Backcalculation of Layer Parameters for LTPP Test Sections, Volume I: Slab on Elastic Solid and Slab on Dense-Liquid Foundation Analysis of Rigid Pavements.* Report FHWA-RD-00-086. FHWA, U.S. Department of Transportation. January 2001.
19. FHWA, U.S. Department of Transportation. *LTPP: Long-Term Pavement Performance Program.* http://www.fhwa.dot.gov/research/tfhrc/programs/infrastructure/pavements/ltpp. Accessed 2013.
20. Papoulis, A., Pillai, S.U. *Probability, random variables and stochastic processes*. McGraw Hill, New York, 1991.

LIST OF TABLES

LIST OF FIGURES

FIGURE 1 (a) Pavement-Vehicle Interaction in a moving coordinate system. Due to dissipative mechanisms in the pavement structure, the wheel is on an upward slope, requiring additional vehicle power to maintain constant speed; (b) Magnified slope under wheel, adapted from Flügge, (*1*).

FIGURE 2 (a) Viscoelastic beam on elastic foundation; (b) Maxwell model to represent viscoelastic behavior of top-layer; (c) deflection obtained from equation (9); (d) deflection under the moving load for different normalized velocities ($\Pi_1 = c/c_{cr}, \Pi_2 = \zeta = \tau(k/m)^{1/2}$).

FIGURE 3 Plots of dimensionless dissipation $\Pi = \frac{\mathcal{D}\ell_s^2 bk}{P^2 c_{cr}}$ in function (a) of dimensionless velocity $\Pi_1 = \frac{c}{c_{cr}}$ at damping ratios, $\Pi_2 = \zeta = \tau(k/m)^{1/2}$ =1, 5, 10; (b) of damping ratio $\Pi_2 = \zeta = \tau(k/m)^{1/2}$ at velocities $\Pi_1 = \frac{c}{c_{cr}}$ 0.11, 0.50 (dash lines are functions fitted to the data proportional to $1/\zeta$); (c) of both invariants $\Pi_1 = \frac{c}{c_{cr}}$ and $\Pi_2 = \zeta$; (d) Absolute error of fitting function (14) for coefficients presented in Table 1.

FIGURE 4 (a) HS20-44 truck used in model calibration/validation; (b) Calibration and (c) Validation of the characteristic relaxation time for an asphalt concrete top-layer on a soil subbase reported in (*5*). (♦) represent values reported by Pouget et al. (*5*). Continuous line represents model prediction of the dissipated energy for the HS20-44 truck.

FIGURE 5 Distributions of (a) top-layer stiffness, E; (b) subgrade stiffness, E_s; (c) top-layer thickness for the different GPS systems considered.

FIGURE 6 Distributions of dissipated energy for the different GPS systems considered, obtained by Monte-Carlo simulations of an HS20-44 truck with axle loads $P_1 = 36.29$ kN (8,000 lbs), $P_2 = P_3 = 145.15$ kN (32,000 lbs) at a constant speed $c = 100$ km/h and a temperature $10℃ \pm 10℃$.

FIGURE 7 Dissipated energy at the 95% confidence level due to a HS20-44 truck with axle loads $P_1 = 36.29$ kN (8,000 lbs), $P_2 = P_3 = 145.15$ kN (32,000 lbs) in function of (a) vehicle speed (at temperature $10℃ \pm 10℃$); and (b) temperature (at constant speed 100 km/h).

TABLE 1 Coefficients p_{ij} (with 95% Confidence Bounds)

i \ j	0	1	2	3	4	5
0	-1.918 (-1.922, -1.915)	4.487 (4.379, 4.596)	-19.54 (-20.64, -18.44)	59.58 (54.61, 64.55)	-92.51 (-102.6, -82.39)	56.23 (48.63, 63.83)
1	-0.4123 (-0.4135, -0.4111)	-1.802 (-1.824, -1.78)	4.014 (3.864, 4.163)	-4.628 (-5.04, -4.217)	1.375 (0.9895, 1.761)	-
2	-0.06942 (-0.06969, -0.06915)	0.2153 (0.2111, 0.2194)	-0.8618 (-0.8794, -0.8441)	0.7344 (0.7124,0.7563)	-	-
3	-0.009575 (-0.009656,-0.009495)	0.0203 (0.0196, 0.021)	0.04669 (0.04542,0.04797)	-	-	-

TABLE 2 GPS Section Categories Based on Pavement Type Considered in our Investigation (*19*)

GPS Number	Pavement Type
GPS-1	Asphalt Concrete Pavement on Granular Base
GPS-2	Asphalt Concrete Pavement on Stabilized Base
GPS-3	Jointed Plane Concrete Pavement
GPS-4	Jointed Reinforced Concrete Pavement
GPS-5	Continuously Reinforced Concrete Pavement
GPS-6	Asphalt Concrete Overlay of Asphalt Concrete Pavement
GPS-7	Asphalt Concrete Overlay of PCC Pavement

TABLE 3 Mean-Value and Standard Deviation for Log-Normal Distribution of Top Layer Stiffness E (in Ln(Mpa)) Subgrade Shear Modulus G_s (in Ln(Mpa)) and Top Layer Thickness h (in Ln(M)) for Considered GPS-Section Categories. To Translate the Subgrade Shear Modulus G_s to the Subgrade Modulus k (or Coefficient of Subgrade Reaction), We Use an Empirical Relation Developed in (*18*): $k = 2\alpha(1+\nu_s)\,G_s$, Where $\alpha = 0.29/m$, $\nu_s = 0.4$ (Poisson's Ratio of Subgrade Assumed Constant for All Sections)

GPS-number	$\mu_{LN}(E)$	$\sigma_{LN}(E)$	$\mu_{LN}(G_s)$	$\sigma_{LN}(G_s)$	$\mu_{LN}(h)$	$\sigma_{LN}(h)$
GPS-1	8.9491	0.6632	5.4393	0.5285	-1.8524	0.5718
GPS-2	9.0151	0.6378	5.7375	0.4997	-1.7556	0.5618
GPS-3	10.4086	0.2540	5.3498	0.3705	-1.4048	0.1079
GPS-4	10.4603	0.1588	5.4723	0.2636	-1.3684	0.0515
GPS-5	10.3903	0.2485	5.5017	0.3805	-1.5135	0.0892
GPS-6	9.0928	0.9506	6.0642	0.6308	-1.4827	0.5278
GPS-7	9.1184	0.8796	6.7312	0.7609	-1.4297	0.2233

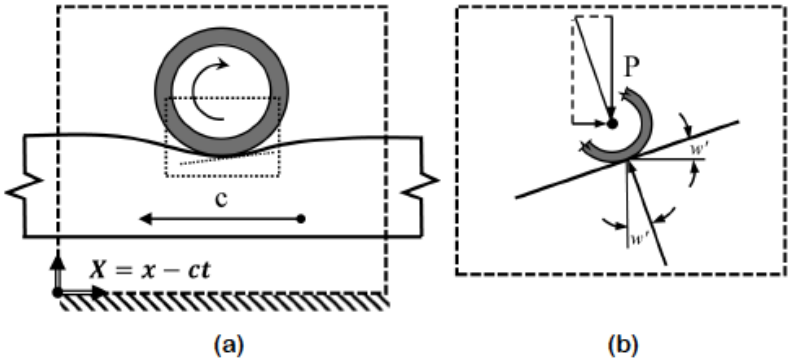

FIGURE 1 (a) Pavement-Vehicle Interaction in a moving coordinate system. Due to dissipative mechanisms in the pavement structure, the wheel is on an upward slope, requiring additional vehicle power to maintain constant speed; (b) Magnified slope under wheel, adapted from Flügge, (*1*).

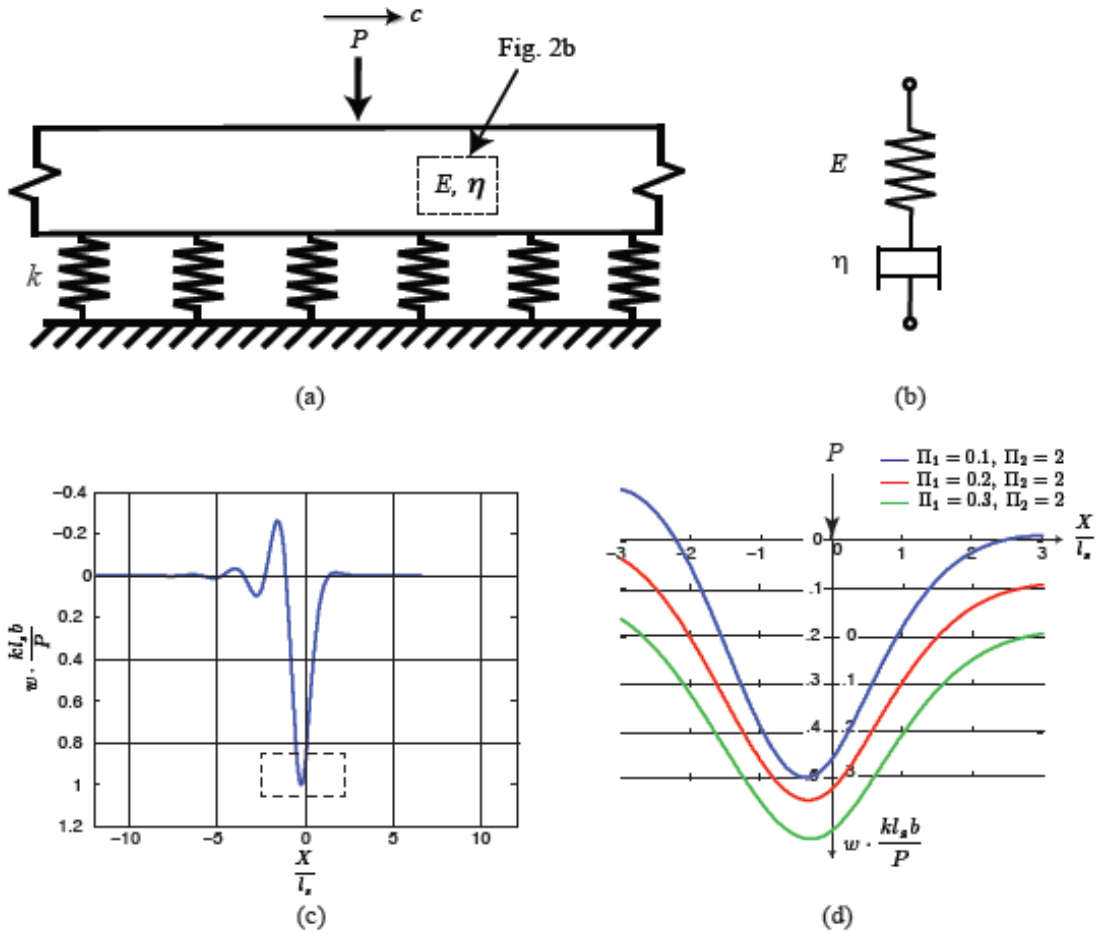

FIGURE 2 (a) Viscoelastic beam on elastic foundation; (b) Maxwell model to represent viscoelastic behavior of top-layer; (c) deflection obtained from equation (9); (d) deflection under the moving load for different normalized velocities ($\Pi_1 = c/c_{cr}, \Pi_2 = \zeta = \tau(k/m)^{1/2}$).

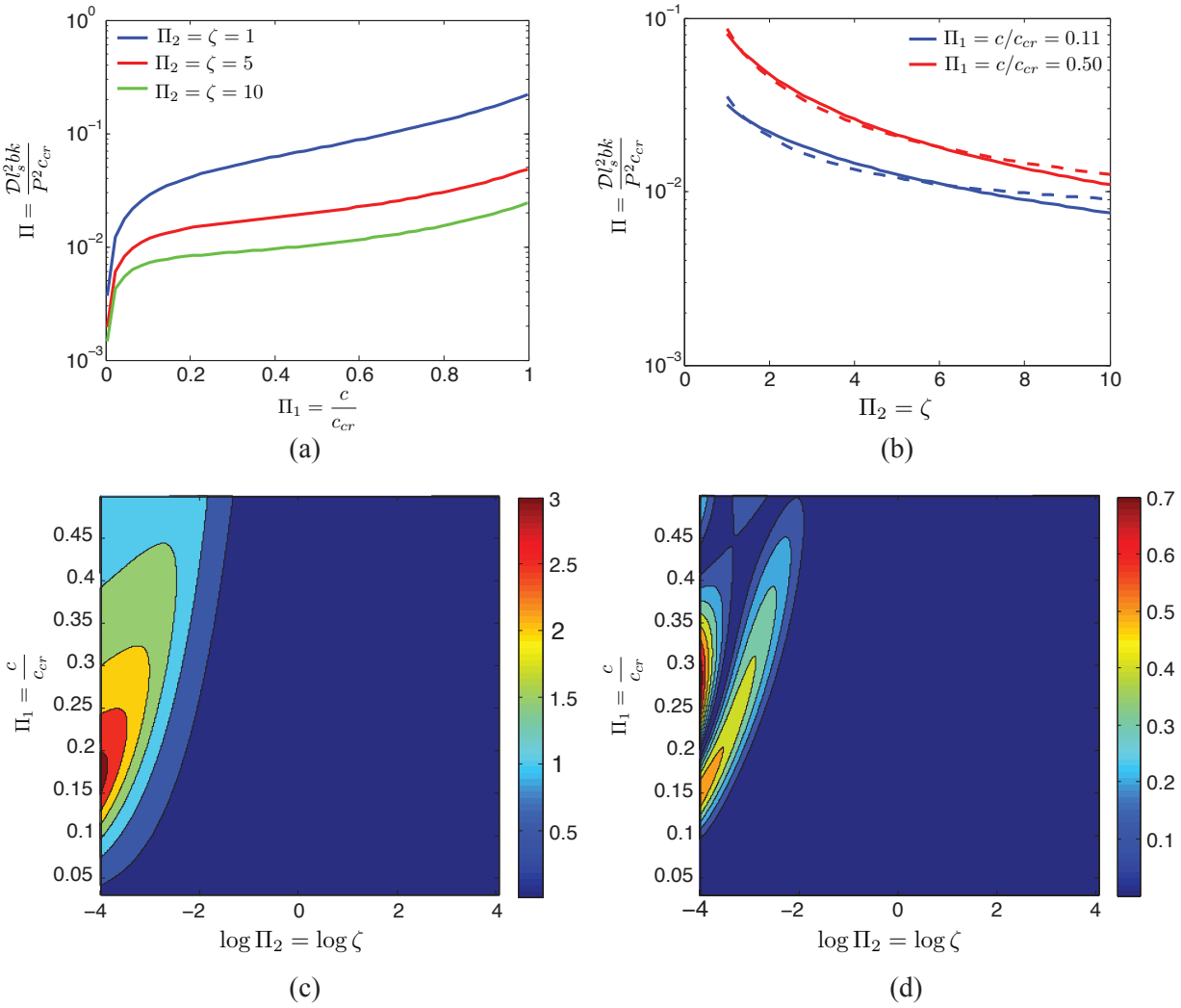

FIGURE 3 Plots of dimensionless dissipation $\Pi = \frac{\mathcal{D}\ell_s^2 bk}{P^2 c_{cr}}$ in function (a) of dimensionless velocity $\Pi_1 = \frac{c}{c_{cr}}$ at damping ratios, $\Pi_2 = \zeta = \tau(k/m)^{1/2}$ =1, 5, 10; (b) of damping ratio $\Pi_2 = \zeta = \tau(k/m)^{1/2}$ at velocities $\Pi_1 = \frac{c}{c_{cr}}$ 0.11, 0.50 (dash lines are functions fitted to the data proportional to $1/\zeta$); (c) of both invariants $\Pi_1 = \frac{c}{c_{cr}}$ and $\Pi_2 = \zeta$; (d) Absolute error of fitting function (14) for coefficients presented in Table 1.

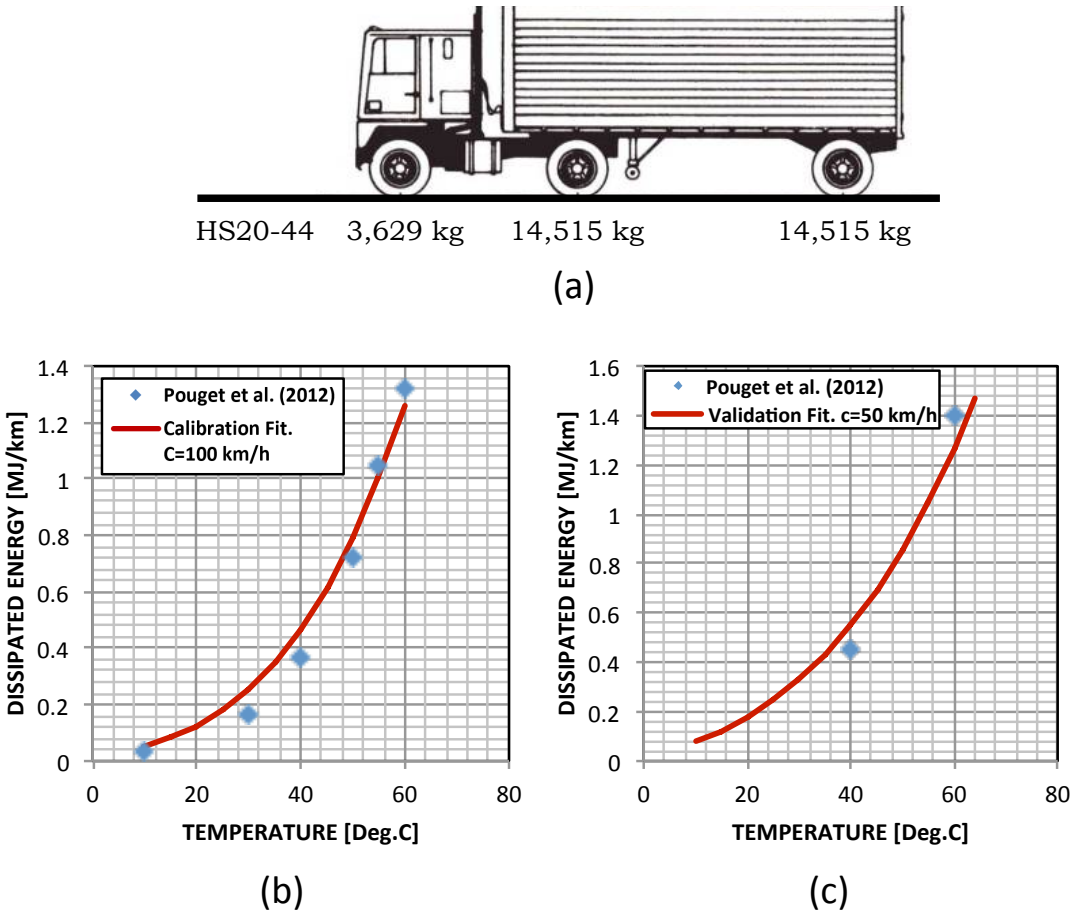

FIGURE 4 (a) HS20-44 truck used in model calibration/validation; (b) Calibration and (c) Validation of the characteristic relaxation time for an asphalt concrete top-layer on a soil subbase reported in (*5*). (♦) represent values reported by Pouget et al. (*5*). Continuous line represents model prediction of the dissipated energy for the HS20-44 truck.

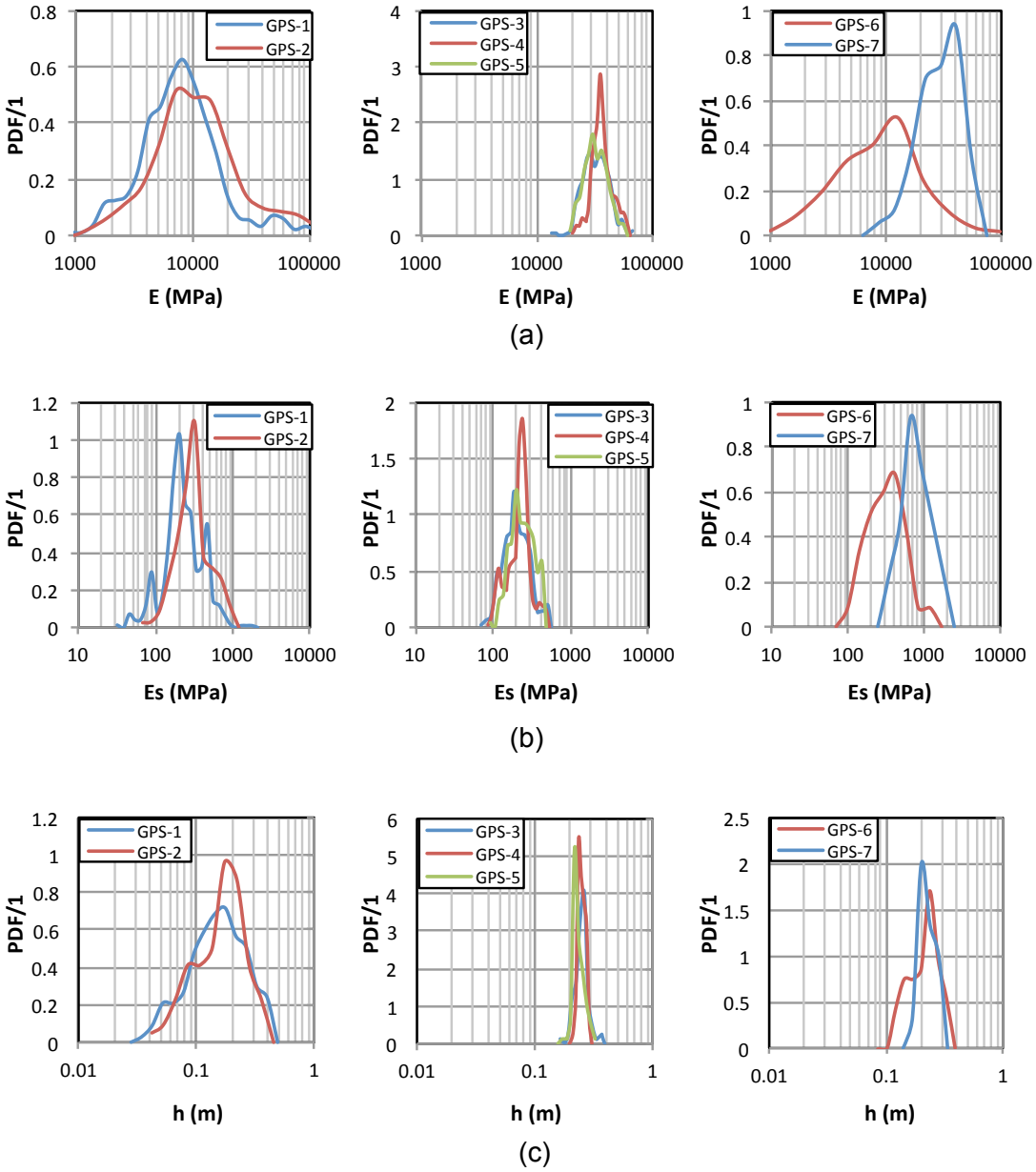

FIGURE 5 Distributions of (a) top-layer stiffness, E; (b) subgrade stiffness, E_s; (c) top-layer thickness for the different GPS systems considered.

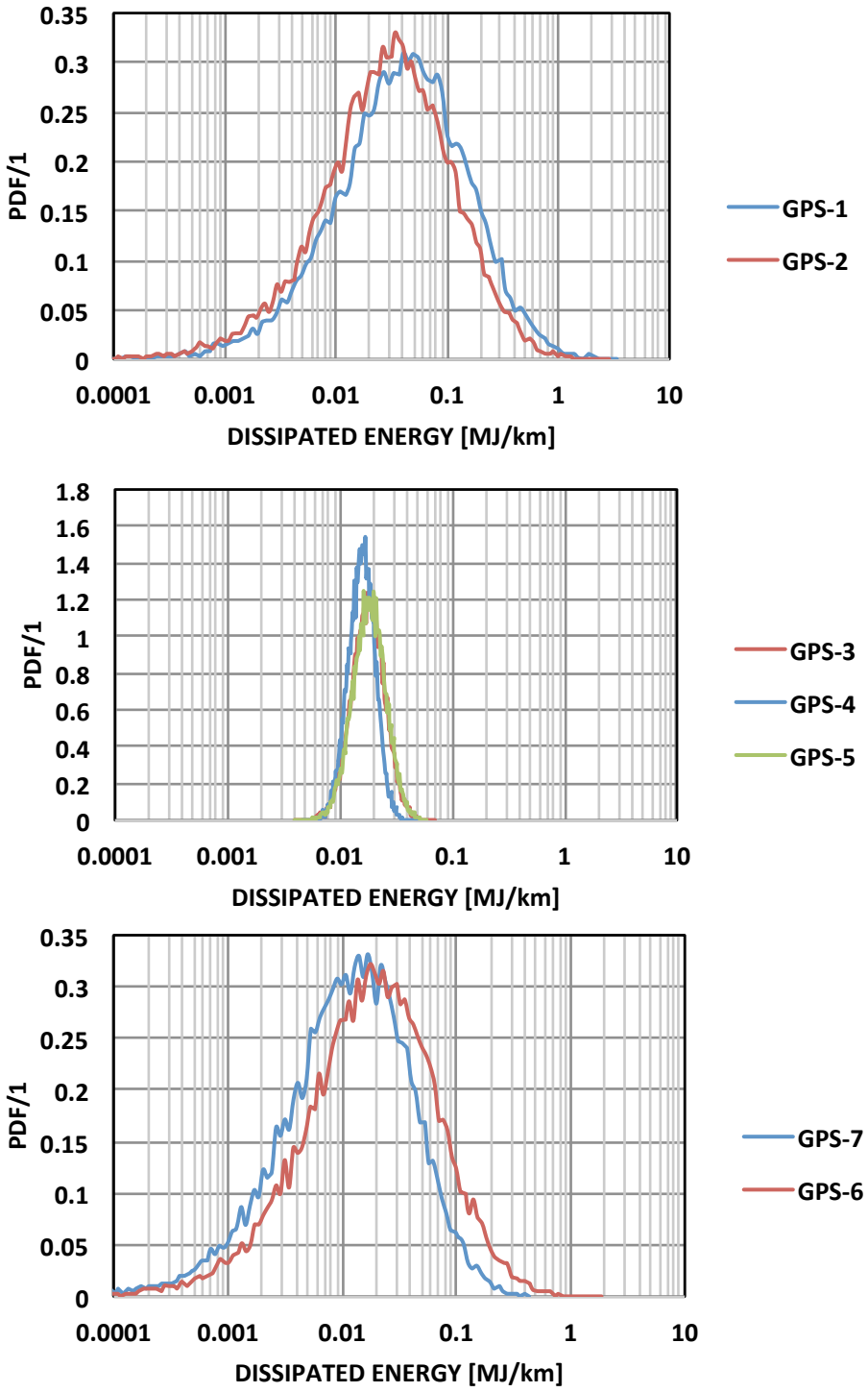

FIGURE 6 Distributions of dissipated energy for the different GPS systems considered, obtained by Monte-Carlo simulations of an HS20-44 truck with axle loads $P_1 = 36.29$ kN (8,000 lbs), $P_2 = P_3 = 145.15$ kN (32,000 lbs) at a constant speed $c = 100$ km/h and a temperature $10℃ \pm 10℃$.

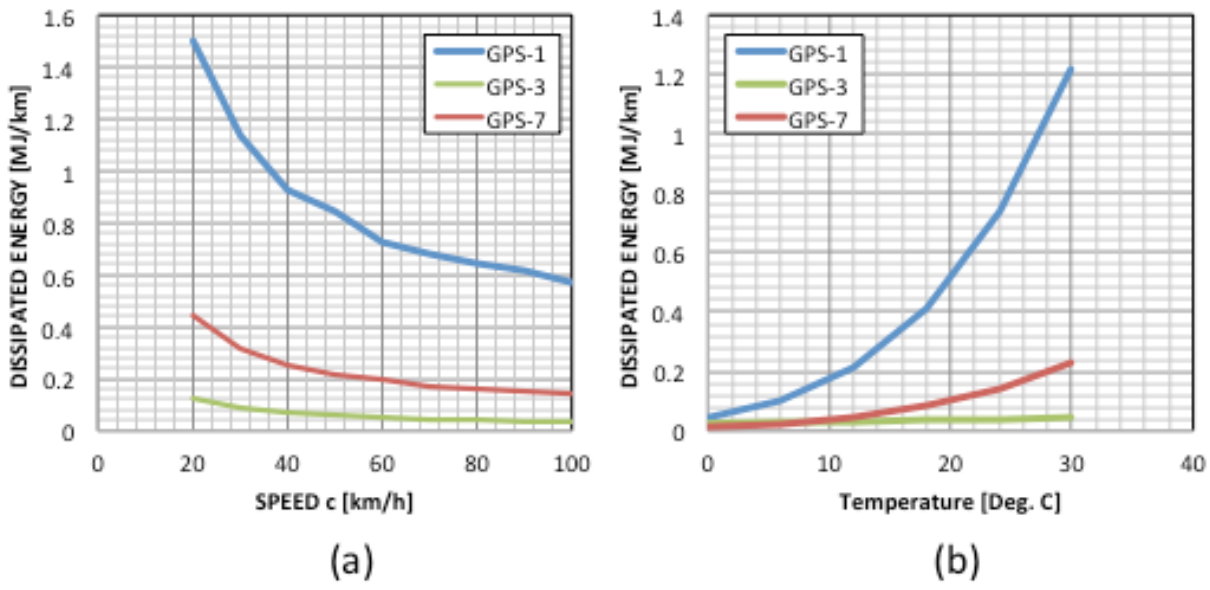

FIGURE 7 Dissipated energy at the 95% confidence level due to a HS20-44 truck with axle loads $P_1 = 36.29$ kN (8,000 lbs), $P_2 = P_3 = 145.15$ kN (32,000 lbs) in function of (a) vehicle speed (at temperature $10℃ \pm 10℃$); and (b) temperature (at constant speed 100 km/h).